Spin reorientation transitions of ultrathin Co/Pd(111) films induced by chemisorption: x-ray magnetic circular dichroism study

2003 J. Phys.: Condens. Matter 15 S537

(http://iopscience.iop.org/0953-8984/15/5/308)

INSTITUTE OF PHYSICS PUBLISHING JOURNAL OF PHYSICS: CONDENSED MATTER

J. Phys.: Condens. Matter **15** (2003) S537–S546 PII: S0953-8984(03)55909-4

Spin reorientation transitions of ultrathin Co/Pd(111) films induced by chemisorption: x-ray magnetic circular dichroism study

Toshihiko Yokoyama[1,3], **Daiju Matsumura**[2], **Kenta Amemiya**[2], **Soichiro Kitagawa**[2], **Norihiro Suzuki**[2] **and Toshiaki Ohta**[2]

[1] Institute for Molecular Science, Myodaiji-cho, Okazaki, Aichi 444-8585, Japan
[2] Department of Chemistry, Graduate School of Science, The University of Tokyo, 7-3-1 Hongo, Bunkyo-ku, Tokyo 113-0033, Japan

E-mail: yokoyama@ims.ac.jp

Received 11 November 2002
Published 27 January 2003
Online at stacks.iop.org/JPhysCM/15/S537

Abstract

Spin reorientation transitions (SRTs) of ultrathin Co/Pd(111) films induced by adsorption of atoms and molecules have been investigated by means of Co $L_{III,II}$-edge x-ray magnetic circular dichroism (XMCD). We have examined CO, NO, O and H as chemisorbed species. We observed the adsorbate-induced SRT from surface parallel to perpendicular magnetization at 200 K in the cases of CO and NO on 4.5 ML Co/Pd(111), while O or H adsorption has been found not to lead to the transition on 4.5 ML Co. We have investigated the detailed Co-thickness dependence in the case of CO and have found that the critical thickness of the SRT in CO-adsorbed Co is ∼6.5 ML, which is greater by ∼3 ML than that of clean Co (∼3.5 ML). From the sum rule analysis, it has been found that the surface parallel orbital moment is reduced after CO adsorption, while the surface normal orbital moment is left unchanged. We can conclude that the observed stabilization of perpendicular magnetic anisotropy due to adsorption is ascribed to quenching of the surface parallel magnetic orbital moment.

1. Introduction

1.1. Magnetic anisotropy of ultrathin films

Magnetic anisotropy of ultrathin films has widely been investigated in recent years [1–5]. Especially, perpendicular magnetic anisotropy (PMA) has attracted great interest from the viewpoints of fundamental physics as well as of technological applications. When one considers the easy axis of thin film magnets, one may conclude that the in-plane magnetization

[3] Author to whom any correspondence should be addressed.

0953-8984/03/050537+10$30.00

would always be energetically favoured if only classical magnetic dipole–dipole interaction were taken into account. This is not always true since several epitaxial magnetic films have been reported to show PMA. PMA is also technologically important since this enables us to exploit new recording media with much higher densities than the present hard disks using in-plane magnetization.

The direction of the easy axis of magnetic films is influenced by the surface, the interface and the volume elastic strains in epitaxial growth of the films on single-crystalline substrates [6]. The microscopic origin of magnetic anisotropy is regarded as spin–orbit interaction [7, 8]. Although the spin magnetic moments dominate the magnetization of materials, exchange interaction between spins is in general described as a scalar product between the spin angular momenta multiplied by a constant exchange interaction, and is therefore not anisotropic. In contrast, the orbital magnetic moment is anisotropic, as long as the atom of interest does not locate in the spherical symmetry. The spin angular momentum interacts with the orbital angular momentum within the atom through the spin–orbit interaction, this leading to the alignment of the orbital and spin magnetic moments. It is noted that although the absolute value of the orbital moment in 3d metals is usually much smaller than that of the spin magnetic moment, the direction of the easy axis is dominated by the orbital magnetic moment. In order to understand magnetic anisotropy of materials from the microscopic point of view, information on the orbital magnetic moment is thus indispensable.

In this work, we have employed ultrathin Co films on Pd(111). Thin Co layers sandwiched between nonmagnetic metals such as Pd(111), Pt(111) and Au(111) are known to exhibit strong PMA [9–13]. Below the critical thickness (typically 5–10 ML), Co layers show a perpendicular magnetic easy axis. Numerous experimental and theoretical studies have revealed that the origin of the perpendicular easy axis is directly related to the interface anisotropy [9–18]. This consequence is reasonable since single-layer Co films show weaker PMA (the critical thickness of $\sim$3.5 ML) [6] than the sandwiched multilayer films. Some electronic interaction between Co and nonmagnetic metals may induce the perpendicular orbital magnetic moments, leading to the stabilization of PMA.

1.2. X-ray magnetic circular dichroism

The x-ray magnetic circular dichroism (XMCD) technique is one of the most suitable methods to investigate the microscopic origin of magnetic anisotropy since the technique provides direct information on the orbital magnetic moment [5, 8]. The circularly polarized x-rays are now available in synchrotron radiation facilities not only from bending magnets or from insertion devices of undulators. The x-ray absorption coefficients of magnetic materials are different between the left- and right-circularly polarized x-rays, depending on whether the magnetization direction is parallel or antiparallel to the helicity of the x-rays. Here, the helicity is a scalar product of unit vectors along the photon spin and the propagation direction of the x-rays. The XMCD is defined as the difference of the absorption coefficients of the magnetic materials between the left- and right-circularly polarized x-rays. When it is difficult to change x-ray helicities, one can also change magnetization directions, this being essentially equivalent to the helicity reversal procedure for the XMCD measurements.

The XMCD technique is element specific since excited electrons are in the deep core levels. We can thus obtain information on the magnetization of each element separately, in contrast to most other techniques for the magnetization measurements. Moreover, so-called XMCD sum rules are known [19, 20]. The first sum rule [19] is to determine the orbital magnetic moment, which is very difficult to obtain by other techniques. The second one is the spin sum rule [20]. This is available when the spin–orbit interaction of the core level investigated is large enough

to separate resonance energies of the two subshell excitations. As a consequence, the two sum rules allow us to determine the orbital and spin magnetic moments separately. Especially, $L_{III,II}$-edge XMCD in 3d elements and $M_{V,IV}$-edge XMCD in lanthanides are useful, because 2p (or 3d) core electrons are excited to the 3d (4f) levels, which are the principal origins of the magnetization.

The XMCD measurements were performed on sandwiched Co films [10, 15], and large perpendicular orbital moments in Co multilayer films were observed compared to that in bulk Co. It was concluded that the strong anisotropy of the Co orbital moments stabilizes the PMA. Another experimental study using the standing-wave method clarified that the orbital moment is actually enhanced in the vicinity of the interface between Co and the substrate [16]. These findings are consistent with theoretical predictions [17, 18].

1.3. Effect of adsorption of atoms and molecules

The effect of adsorption of atoms and molecules on the magnetic easy axis is also an interesting subject. It was revealed by means of the magneto-optical Kerr effect (MOKE) [21, 22] that PMA of the Ni/Cu(001) system [23] is stabilized when the surface is covered with CO or H. The clean Ni/Cu(001) film shows PMA in the thickness range from 11 to ∼50 ML and exhibits in-plane magnetization below 11 ML and above 50 ML. The critical thickness of 11 ML for clean Ni/Cu(001) was found to be lowered to ∼7 ML upon H or CO adsorption. This implies that slightly below the critical thickness such as 8–10 ML, a spin reorientation transition (SRT) takes place from the surface parallel to the perpendicular direction upon adsorption of CO or H. It was concluded that the contribution of the surface anisotropy, which favours parallel magnetization, is significantly reduced due to the interaction between surface Ni and the adsorbates.

Other examples of the rotation of the easy axis induced by gas adsorption have been reported in systems such as CO/Co/Pt(111) [24], CO/Co/Cu(110) [25, 26], CO, H, O/Fe/W(110) [27] and O/Fe/Ag(001) [28]. H/Fe/Cu(001) also shows SRT induced by H adsorption [29], although in this case H adsorption results in the structural transformation of the Fe film itself, and the change in the surface anisotropy might be a minor effect. In order to elucidate the origin of the mechanism of these SRTs from a microscopic viewpoint, it is necessary to directly measure the orbital magnetic moment that determines the magnetic easy axis. For this purpose, the XMCD technique should be the most suitable method.

Here, we report the effect of gas adsorption on the magnetic easy axis of Co/Pd(111) by means of Co $L_{III,II}$-edge XMCD measurements. As chemisorbed species, we have examined CO, NO, H and O. CO is one of the most popular chemisorption gases and adsorbs in atop sites as well as in bridge sites of the Co surface with the molecular axis perpendicular to the surface. Previously, we reported induced magnetic moments in CO and NO adsorbed on Ni and Co films by measuring adsorbate K-edge XMCD [30–34]. In this work, we have discovered SRT of Co/Pd(111) induced by CO [35] and NO adsorption at 200 K, while H or O adsorption does not lead to SRT.

2. Experimental details

2.1. Sample preparation

A Pd(111) single crystal was cleaned by repeated cycles of Ar^+ sputtering (2 keV) and annealing at ∼1070 K in an ultrahigh-vacuum chamber for the XMCD measurements. Sample annealing was performed by electron bombardment from the rear side of the crystal,

and the temperature was monitored with a chromel–alumel thermocouple. The crystal order at the surface was verified by LEED (low-energy electron diffraction) and RHEED (reflection high-energy electron diffraction), and the cleanliness of the surface was confirmed by NEXAFS (near-edge x-ray-absorption fine structure) and AES (Auger electron spectroscopy).

Co thin films were deposited on clean and ordered Pd(111) at room temperature with the electron-beam evaporation method. The thickness of the films was calibrated by the AES intensity ratio between Co and Pd. The RHEED oscillations, which are usually useful for the estimation of the thickness of epitaxial films on single-crystal surfaces, were too weak to yield reliable estimation of the thickness.

The Co/Pd(111) films were subsequently dosed with appropriate amounts of CO, NO, O_2 or H_2 at 200 K. Typical amounts of dosage were ∼4 L (1 L = 10^{-6} Torr s; 1 Torr = 133 Pa), which sufficiently reached saturated adsorption in the cases of CO, NO and H. In the O adsorption, oxidation to inner Co layers proceeds during prolonged O_2 dosage. We have checked O K- and Co L-edge NEXAFS spectra by performing stepwise dosage of O_2 to distinguish the O-adsorbed state from the oxidized one. Although details of the procedure are not described here, we came to the conclusion that the 3 L dosage yielded the O-adsorbed phase, while the 24 L one gave a surface oxidized film.

2.2. XMCD measurements

The Co $L_{III,II}$-edge XMCD spectra were taken at the bending-magnet station Beamline 7 A of the Photon Factory at the Institute of Materials Structure Science, High-Energy Accelerator Research Organization (KEK-PF) [36]. Circularly polarized x-rays were obtained by using x-rays above (0.4 ± 0.1 mrad, positive helicity) or below (-0.4 ± 0.1 mrad, negative helicity) the synchrotron orbit plane. The circular polarization factor P_c was estimated to be 0.80 by measuring the Co $L_{III,II}$-edge XMCD spectra of bulk Co prepared *in situ*. All the spectra were recorded in a partial-electron-yield mode using a detector consisting of a 25 mm diameter microchannel plate (MCP) and two Au-coated W grids; this detector was placed below the sample. To enhance the surface-to-bulk ratio of the signals, the solid angle was limited so that it would collect electrons with grazing emission only. A retarding voltage of −500 V was applied to the second grid (closer to the MCP), while the first one was grounded. The intensity of the incident x-rays I_0 was monitored simultaneously with an Au-coated W mesh placed upstream of the sample.

The XMCD spectra were obtained by reversing the magnetization of the films or the helicity of the incident x-rays. The sample was mounted in a Helmholtz coil and was magnetized by a current pulse (∼0.1 T) along the incident x-rays. The remanent magnetization was examined. For the detection of magnetization, XMCD measurements were performed at grazing ($\theta = 30°$) and normal ($\theta = 90°$) x-ray incidence. Here θ is the x-ray incident angle between the electric field vector of x-rays and the surface normal. The measurement temperature was 200 K in all cases.

3. Results

3.1. CO/Co/Pd(111)

Figure 1 shows the Co $L_{III,II}$-edge circularly polarized spectra and XMCD of the clean and CO-adsorbed 4.5 ML Co film grown on Pd(111). The XMCD spectra were obtained by the formula $(\mu^{\uparrow\uparrow} - \mu^{\uparrow\downarrow})/P_c$, where $\mu^{\uparrow\uparrow}$ and $\mu^{\uparrow\downarrow}$ are the circularly polarized spectra with the photon helicity parallel and antiparallel, respectively, to the majority spin of the sample.

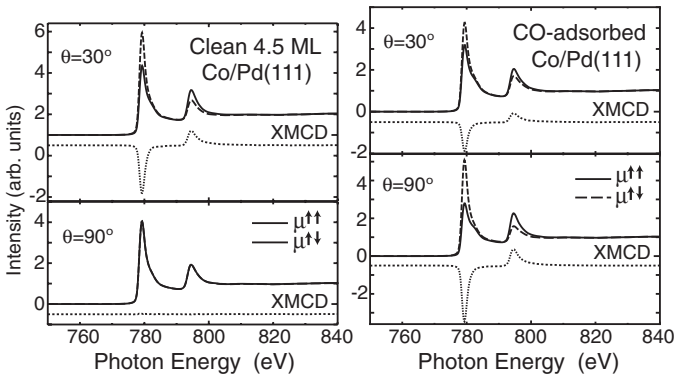

Figure 1. Co $L_{III,II}$-edge circularly polarized x-ray absorption (soild and dashed curves) and XMCD (dotted curves) spectra of 4.5 ML Co/Pd(111) before (left) and after (right) CO adsorption at 200 K. The spectra were taken at the x-ray incident angles θ of 30° (grazing) and 90° (normal), and the measurement temperatures were also 200 K. Remanent magnetization was examined.

$\mu^{\uparrow\uparrow}$ and $\mu^{\uparrow\downarrow}$ were calculated by dividing the raw partial-electron-yield spectra by the I_0 function measured simultaneously, subsequent pre-edge linear background subtraction, normalization with the edge jumps and consequent correction of the self-absorption effect [37]. In clean 4.5 ML Co/Pd(111), strong XMCD signals were observed at grazing x-ray incidence, while no XMCD signal is observed at normal incidence. This implies that the easy axis of the films lies parallel to the surface since the remanent magnetization was investigated. By dosing the Co film with saturated amounts of CO at 200 K, the spectra have changed drastically. The XMCD signal appears at normal x-ray incidence, implying the occurrence of SRT by CO adsorption.

Our quantitative evaluation uses the well established XMCD sum rules for the L edge [19, 20]:

$$m_l = -\frac{4}{3}\frac{n_h \mu_B}{P_c \cos\chi}\frac{\int_{L_{III}+L_{II}}(\mu^{\uparrow\uparrow}-\mu^{\uparrow\downarrow})\,\mathrm{d}E}{\int_{L_{III}+L_{II}}(\mu^{\uparrow\uparrow}+\mu^{\uparrow\downarrow}-2\mu^{BG})\,\mathrm{d}E}$$

and

$$m_s = -\frac{2n_h \mu_B}{P_c \cos\chi}\frac{\int_{L_{III}}(\mu^{\uparrow\uparrow}-\mu^{\uparrow\downarrow})\,\mathrm{d}E - 2\int_{L_{II}}(\mu^{\uparrow\uparrow}-\mu^{\uparrow\downarrow})\,\mathrm{d}E}{\int_{L_{III}+L_{II}}(\mu^{\uparrow\uparrow}+\mu^{\uparrow\downarrow}-2\mu^{BG})\,\mathrm{d}E} + 7\langle T_z\rangle\mu_B,$$

where m_l and m_s are the orbital and spin magnetic moments, n_h the 3d hole number, μ_B the Bohr magneton, χ the angle between the magnetization and the wavevector of the incident x-rays, μ^{BG} the background absorption and $\langle T_z\rangle$ the magnetic dipole moment. The 3d hole numbers n_h in the present Co thin films were obtained by comparing the white-line intensities with the bulk ones and using $n_h = 2.5$ of bulk Co [38]. Since the magnetic dipole term $\langle T_z\rangle$ was not taken into account in the present analysis, the obtained spin magnetic moment is effective ($m_s^{eff} = m_s + 7\langle T_z\rangle$). Although the absolute values of the magnetic moments obtained here might contain some ambiguities, we will focus our attention only on the relative magnitudes of the magnetic moments in the following discussion.

Figure 2(a) shows the projected magnetization of clean Co/Pd(111) at 200 K with various Co thicknesses for the surface normal and parallel directions, which is obtained from the spin sum rule given above. Below ∼3 ML, the film shows perpendicular magnetization, while above ∼4 ML the film exhibits surface parallel magnetization. Thus, the critical thickness is ∼3.5 ML, the same as it was for 300 K in the previous report [14]. The 1.5 ML Co film

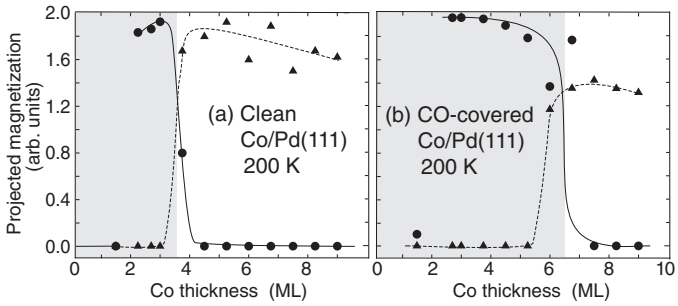

Figure 2. Effective spin magnetic moments of (a) clean and (b) CO-covered Co films on Pd(111) at 200 K as a function of Co thickness. Circles and solid curves correspond to the surface normal direction, while triangles and dashed curves correspond to the surface parallel one. Hatched areas indicate the PMA regions.

shows no magnetization in either direction, implying the Curie temperature below 200 K. In the case shown in figure 1, the 4.5 ML Co film inherently gives a parallel magnetic easy axis, and undergoes SRT from the in-plane to perpendicular direction upon CO adsorption. The effective spin magnetic moments of CO-adsorbed Co/Pd(111) are plotted in figure 2(b) as a function of Co thickness. One can see that films thinner than ∼6.5 ML exhibit PMA. The critical thickness increases by ∼3 ML compared to that of the clean surface films (∼3.5 ML) in figure 2(a).

To obtain microscopic understanding of SRT, we show figure 3, that gives the changes in the effective orbital magnetic moments in Co/Pd(111) induced by CO adsorption. Here, 'effective' means that the orbital magnetic moments given in figure 3 are obtained without taking the temperature effect (reduction due to finite T/T_C) into account. Note also that although all the measurement temperatures were 200 K, the Curie temperature T_C might be somewhat different between clean and CO-adsorbed films. We have neglected these effects in figure 3. Uncertainties due to the temperature effect are, however, much smaller than the observed differences. From the viewpoint of the magnetic easy axis, we can classify Co thickness into three regions. Below 3 ML, Co films show perpendicular magnetization even before CO adsorption (region I). Above 7 ML, on the other hand, Co films show parallel magnetization even after CO adsorption (region III). In the thickness range between 3 and 7 ML, Co films exhibit SRT (region II). As seen in region I, the perpendicular orbital magnetic moments are left unchanged upon CO adsorption. In region II, the orbital magnetic moment after CO adsorption (perpendicular magnetization) is greater than that before CO adsorption (parallel). In region III, adsorption of CO causes reduction of the parallel orbital magnetic moments.

3.2. NO, O and H adsorption on Co/Pd(111)

Figure 4 shows the Co $L_{III,II}$-edge XMCD spectra of the NO- and H-adsorbed 4.5 ML Co/Pd(111). The clean 4.5 ML Co/Pd(111) shows in-plane magnetization, as shown in figure 1. Upon NO adsorption, the XMCD signal predominantly appears in the normal incidence spectra, implying the occurrence of SRT as in the case of CO adsorption. The reduction of the XMCD intensity is however found to be significant in the NO case, if one compares the spectra in figures 1 and 4. A similar sum-rule analysis was performed and we found a significant reduction of the magnetization: the perpendicular magnetization for NO-adsorbed Co/Pd(111) is as small as 56% of the in-plane magnetization for clean Co. These results are consistent

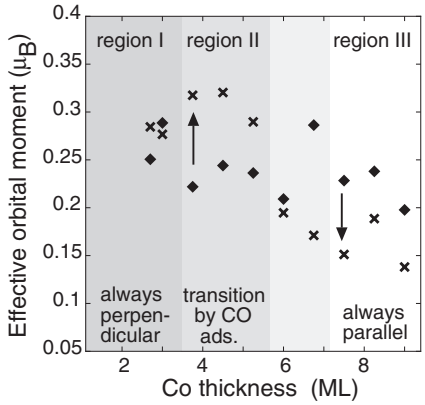

Figure 3. Effective orbital magnetic moments of the Co films on Pd(111) at 200 K as a function of Co thickness. Here, 'effective' means that the orbital magnetic moments are obtained without taking the temperature effect (see the text for details). Diamonds and crosses denote clean and CO-adsorbed Co, respectively. Note that there exists a mixture phase between regions II and III, where the perpendicular or parallel orbital moment is poorly defined.

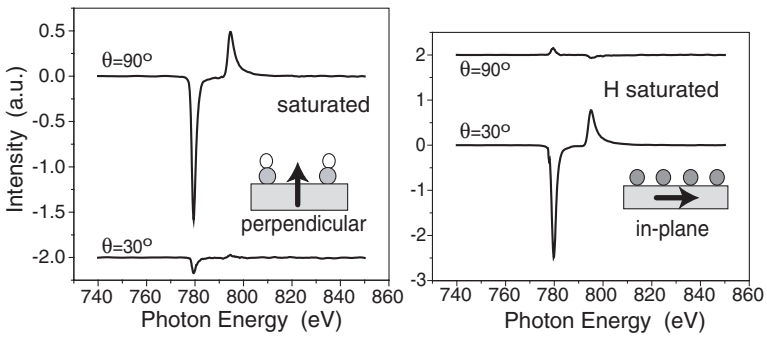

Figure 4. Co $L_{III,II}$-edge XMCD spectra of 4.5 ML Co/Pd(111) after adsorption of saturated amounts of NO (left) and H (right) at 200 K. The spectra were taken at the x-ray incident angles θ of 30° (grazing) and 90° (normal), and the measurement temperatures were also 200 K. Remanent magnetization was examined.

with our previous study on NO/Co/Cu(001) [35], and NO is regarded as an effective killer of the substrate magnetization. Such significant reduction of the Co spin magnetic moment indicates strong antiferromagnetic coupling between NO $2\pi^*$ and Co 3d electrons.

In contrast, in H-adsorbed Co/Pd(111), the XMCD signal shows in-plane magnetization, implying that H adsorption does not induce SRT of 4.5 ML Co/Pd(111). This is in good contrast to the case of H/Ni/Cu(001), which shows SRT when the Ni thickness is in the range of 7–10 ML, irrespective of CO or H [21, 22, 36]. One possible reason for such a difference between Co/Pd(111) and Ni/Cu(001) may be the difference in the H coverage. Although H coverage is difficult to estimate, it is expected to be much smaller than the Ni/Cu(001) case, where the saturation coverage is as much as 1 ML [38].

Figure 5 shows the Co $L_{III,II}$-edge XMCD spectra of the 4.5 ML Co/Pd(111) exposed to 3 and 24 L O_2 at 200 K. As described in the previous section, from the numbers of the O K-edge jumps and Co L-edge spectral features by varying the dosage from 1 to 24 L (figures not shown), it can be remarked that the film exposed to 3 L O_2 gives O-adsorbed Co/Pd(111),

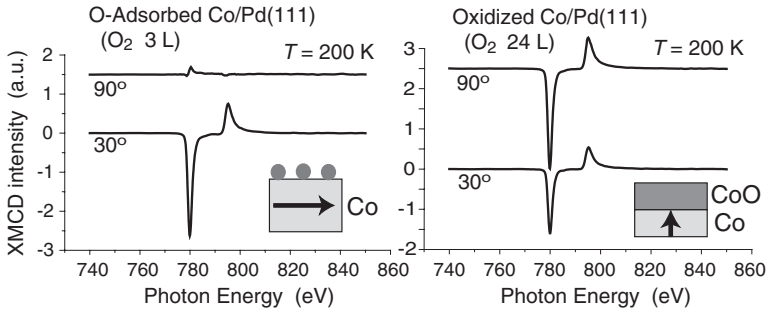

Figure 5. Co $L_{III,II}$-edge XMCD spectra of 4.5 ML Co/Pd(111) exposed to 3 L (left) and 24 L (right) O_2 at 200 K. The spectra were taken at the x-ray incident angles θ of 30° (grazing) and 90° (normal), and the measurement temperatures were also 200 K. Remanent magnetization was examined. The films exposed to 3 and 24 L O_2 can be regarded as the O-adsorbed and surface-oxidized films, respectively.

while 24 L O_2 dosage yields an oxide-covered film. Accordingly, we can conclude from the XMCD spectra that O adsorption does not lead to SRT of the 4.5 ML Co/Pd(111), being similar to the case of H/Co/Pd(111). As the amounts of deposited oxygen increase, however, the film becomes perpendicularly magnetized. This should be because the actual thickness of Co metal becomes smaller by converting the surface layers to CoO.

4. Remaining problems

Although the microscopic origin of SRT induced by CO and NO can be ascribed to quenching of the in-plane orbital magnetic moment of the surface Co atoms, there seem to remain several open problems that should be clarified in future works. As for the structure of metal thin films, 9% of the lattice mismatch exists in Co/Pd(111). Although non-pseudomorphic growth was observed by means of RHEED [14], the EXAFS (extended x-ray-absorption fine-structure) study [40] indicated the presence of strain originating from the lattice mismatch in a few ML films. The structure of the Co films on Pd(111) is not well understood. Since the magnetoelastic anisotropy induced by pseudomorphic growth is the key to PMA for Ni/Cu(001) [23], it must also be important to consider the structure of the Co thin film. Intermixing at the interface is another possibility to explain magnetic anisotropy, because a recent experiment pointed out the formation of alloy structure in the Co/Pd interface [41]. In this study, we cannot discuss the effects of film structures on magnetic anisotropy. However, since the surface tension of the film would relax in a few monolayers, we can rule out the possibility of structural change of the films for determining the easy axis of the Co thin films. The complexity of the structure at the interface does not allow us to distinguish between the magnetoelastic and magnetocrystalline anisotropies.

In this work, adsorption was conducted at 200 K for all the gases investigated. We have also performed the experiments on CO adsorption on Co/Pd(111) at 300 K. In these experiments, we have not observed a shift in the critical thickness; namely the critical thickness of Co is ∼3.5 ML before and after CO adsorption [35]. Although the saturation coverage of CO at 300 K is lower than at 200 K, it is greater than the critical CO coverage at 200 K. This cannot be understood. The possibility of a different CO adsorption site on the surface cannot be ruled out. For CO adsorption on hcp Co(0001), it has been reported that CO adsorbs on both atop and bridge sites at 180 K [42], and theoretical calculations have predicted differences

in magnetic interactions at different adsorption sites [43]. The adsorption site of CO on the present Co/Pd(111) films has not been determined yet. These microscopic explanations of surface and interface magnetic states may thus be a subject of future studies.

5. Conclusions

We have investigated the effects of adsorption on the magnetic easy axis in Co/Pd(111) by using XMCD. We have found that PMA is stabilized by adsorption of CO and NO on Co/Pd(111) at 200 K and that the critical thickness increases by about 3 ML in the CO case. From the change of orbital moments from before to after adsorption of CO or NO, the stabilization of PMA by CO or NO is attributed to the reduction of the surface parallel magnetic orbital moment. H or O adsorption may not contribute to such effective quenching of the in-plane orbital moments on the surface atoms and does not lead to the stabilization of PMA.

Acknowledgments

The authors acknowledge Professor Baberschke and his group members for their essential advice to construct our XMCD system and for their interest and valuable discussion concerning our works. The present work was performed under the approval of the Photon Factory Program Advisory Committee (PF-PAC No 2001S2-003).

References

[1] Heinrich B and Cochran J F 1993 Ultrathin metallic magnetic films: magnetic anisotropies and exchange interactions *Adv. Phys.* **42** 523
[2] Heinrich B and Bland J A C 1994 *Ultrathin Magnetic Structures* vols 1 and 2 (Berlin: Springer)
[3] Johnson M T, Bloemen P J H, den Broeder F J A and de Vries J J 1996 Magnetic anisotropy in metallic multilayers *Rep. Prog. Phys.* **59** 1409
[4] Farle M 1998 Ferromagnetic resonance of ultrathin metallic layers *Rep. Prog. Phys.* **61** 755
[5] Stöhr J 1999 *J. Magn. Magn. Mater.* **200** 470
[6] Néel L 1954 *J. Physique Radium* **15** 225
Néel L 1954 *J. Physique Radium* **15** 376
[7] van Vleck J H 1937 *Phys. Rev.* **52** 1178
[8] Bruno P 1989 *Phys. Rev.* B **39** 865
[9] Wu Y, Stöhr J, Hermsmeier B D, Samant M G and Weller D 1992 *Phys. Rev. Lett.* **69** 230
[10] Weller D, Wu Y, Stöhr J, Samant M G, Hermsmeier B D and Chappert C 1994 *Phys. Rev.* B **49** 12888
[11] Nakajima N, Koide T, Shidara T, Miyauchi H, Fukutani H, Fujimori A, Iio K, Katayama T, Nývlt M and Suzuki M 1998 *Phys. Rev. Lett.* **81** 5229
[12] Tatnall C J, Schille J P, Grundy P J and Lord D G 1997 *J. Magn. Magn. Mater.* **165** 391
[13] Dürr H A, Dhesi S S, Dudzik E, Knabben D, van der Laan G, Goedkoop J B and Hillebrecht F U 1999 *Phys. Rev.* B **59** R701
[14] Engel B N, Wiedmann M H, Leeuwen R A V and Falco C M 1993 *J. Magn. Magn. Mater.* **126** 532
[15] Koide T, Miyauchi H, Okamoto J, Shidara T, Fujimori A, Amemiya K, Takeshita H, Yuasa S, Katayama T and Suzuki Y 2001 *Phys. Rev. Lett.* **87** 257201
[16] Kim S-K and Kortright J B 2001 *Phys. Rev. Lett.* **86** 1347
[17] López-Urías F, Dorantes-Dávila J and Dreyssé H 1997 *J. Magn. Magn. Mater.* **165** 262
[18] Szunyogh L, Újfalussy B, Bruno P and Weinberger P 1997 *J. Magn. Magn. Mater.* **165** 254
[19] Thole B T, Carra P, Sette F and van der Laan G 1992 *Phys. Rev. Lett.* **68** 1943
[20] Carra P, Thole B T, Altarelli M and Wang X 1993 *Phys. Rev. Lett.* **70** 694
[21] Vollmer R, Gutjahr-Löser Th, Kirschner J, van Dijken S and Poelsema B 1999 *Phys. Rev.* B **60** 6277
[22] van Dijken S, Vollmer R, Poelsema B and Kirschner J 2000 *J. Magn. Magn. Mater.* **210** 316
[23] Schulz B and Baberschke K 1994 *Phys. Rev.* B **50** 13467
[24] Robach O, Quiros C, Steadman P, Peters K F, Lundgren E, Alvarez J, Isern H and Ferrer S 2002 *Phys. Rev.* B **65** 054423

[25] Hope S, Gu E, Choi B and Bland J A C 1998 *Phys. Rev. Lett.* **80** 1750
[26] Hope S, Gu E, Choi B and Bland J A C 1998 *Phys. Rev.* B **57** 7454
[27] Elmer H J, Hauschild J and Gradmann U 1999 *J. Magn. Magn. Mater.* **198/199** 222
[28] Chen J and Erskine J L 1992 *Phys. Rev. Lett.* **68** 1212
[29] Vollmer R and Kirschner J 2000 *Phys. Rev.* B **61** 4146
[30] Yokoyama T, Amemiya K, Miyachi M, Yonamoto Y, Matsumura D and Ohta T 2000 *Phys. Rev.* B **62** 14191
[31] Amemiya K, Yokoyama T, Yonamoto Y, Miyachi M, Kitajima Y and Ohta T 2000 *Japan. J. Appl. Phys.* **39** L63
[32] Amemiya K, Yokoyama T, Yonamoto Y, Matsumura D and Ohta T 2001 *Phys. Rev.* B **64** 132405
[33] Yokoyama T, Amemiya K, Yonamoto Y, Matsumura D and Ohta T 2001 *J. Electron Spectrosc. Relat. Phenom.* **119** 207
[34] Yonamoto Y, Yokoyama T, Amemiya K, Matsumura D, Kitagawa S, Hamada Y, Ohta T and Koide T 2002 *J. Phys. Soc. Japan* **71** 607
[35] Matsumura D, Yokoyama T, Amemiya K, Kitagawa S and Ohta T 2002 *Phys. Rev.* B **66** 024402
[36] Amemiya K, Kondoh H, Yokoyama T and Ohta T 2002 *J. Electron Spectrosc. Relat. Phenom.* **124** 151
[37] Nakajima R, Stöhr J and Idzerda Y U 1999 *Phys. Rev.* B **59** 6421
[38] Eriksson O, Johansson B, Albers R C, Boring A M and Brooks M S S 1990 *Phys. Rev.* B **42** 2707
[39] Christmann K, Schober O, Ertl G and Neumann M 1974 *J. Chem. Phys.* **60** 4528
[40] Kim S-K, Koo Y-M, Chernov V A and Padmore H 1996 *Phys. Rev.* B **53** 11114
[41] Kim S-K, Koo Y-M, Chernov V A, Kortright J B and Shin S C 2000 *Phys. Rev.* B **62** 3025
[42] Lahtinen J, Vaari J and Kauraala K 1998 *Surf. Sci.* **418** 502
[43] Pick Š and Dreyssé H 1999 *Phys. Rev.* B **59** 4195
[44] Amemiya K, Kitajima Y, Ohta T and Ito K 1996 *J. Synchrotron Radiat.* **3** 282
Amemiya K, Kitajima Y, Yonamoto Y, Ohta T, Ito K, Sano K, Nagano T, Koeda M, Sasai H and Harada Y 1997 *Proc. SPIE* **3150** 171
Kitajima Y, Amemiya K, Yonamoto Y, Ohta T, Kikuchi T, Kosuge T, Toyoshima A and Ito K 1998 *J. Synchrotron Radiat.* **5** 729
Kitajima Y, Yonamoto Y, Amemiya K, Tsukabayashi H, Ohta T and Ito K 1999 *J. Electron Spectrosc. Relat. Phenom.* **101–103** 927
[45] Tischer M, Arvanitis D, Yokoyama T, Lederer T, Tröger L and Baberschke K 1994 *Surf. Sci.* **307–309** 1096